AD A095141

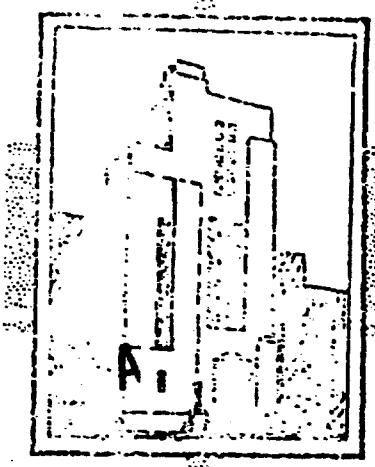

HYDROMECHANICS

o

AERODYNAMICS

o

STRUCTURAL MECHANICS

o

APPLIED MATHEMATICS

AN EXPERIMENTAL INVESTIGATION OF EFFECT OF END CONDITIONS ON STRENGTH OF STIFFENED CYLINDRICAL SHELLS

by

Robert F. Keefe and James A. Overby

DTIC ELECTE JAN 19 1981

[redacted]

DISTRIBUTION STATEMENT A
Approved for public release;
Distribution Unlimited

STRUCTURAL MECHANICS LABORATORY
RESEARCH AND DEVELOPMENT REPORT

December 1979

DTMB Rept. 1326
Report 1326

81 1 09 043

DDC FILE COPY

(Rev. 3-58)

DISCLAIMER NOTICE

THIS DOCUMENT IS BEST QUALITY PRACTICABLE. THE COPY FURNISHED TO DTIC CONTAINED A SIGNIFICANT NUMBER OF PAGES WHICH DO NOT REPRODUCE LEGIBLY.

AN EXPERIMENTAL INVESTIGATION OF EFFECT OF END CONDITIONS ON STRENGTH OF STIFFENED CYLINDRICAL SHELLS

by

Robert F. Keefe and James A. Overby

Accession
NTIS GRA&I
DTIC TAB
UNANNOUNCED

December 1959

Report 1326
NS 731-038

TABLE OF CONTENTS

LIST OF FIGURES

LIST OF TABLES

ABSTRACT

Six pairs of stiffened cylinders, machined from thick tubes and identical except for the size and spacing of the frames at the ends, were subjected to external hydrostatic pressure to establish the adequacy of a design procedure for the end bays. All the cylinders failed by axisymmetric shell yielding, four in the end bay, four in the first full-length bay, and four in the second full-length bay. For each pair of identical cylinders, the locations of damage at failure were identical and the collapse pressures differed by less than 1 percent when adjusted to a common yield strength. Test results indicated that with the end conditions established by the end-bay theory of TMB Report 1065, the collapse pressure could be increased as much as 5 percent and failure could be shifted away from the ends of the cylinder.

INTRODUCTION

In research with stiffened cylindrical shells, failures in the axisymmetric yield mode have invariably occurred in bays adjacent to holding bulkheads at lower pressures than those predicted by "equal strength bay" analysis.

In an effort to counteract the weakening influences of end effects, the David Taylor Model Basin developed the design procedure in Reference 1* to obtain an optimum design by which all stiffeners deflect the same amount at failure and no bay is weakened by the influence of the bulkheads.

To validate the adequacy of the design procedure a series of model tests was initiated to investigate six different end conditions. The general objectives were as follows:

1. To establish the adequacy of the optimum design procedure by observations of collapse pressures.

2. To verify the strain distribution in the end bays as predicted by the optimum design procedure by measurement of strains.

In order that results might serve to verify the established objectives, parameters affecting the collapse pressure and fabrication of these models were carefully controlled. The models, their fabrication and instrumentation, and the model tests are described in this report. In addition, experimental strains, deflections, and collapse pressures are compared with theoretical values.

---

*References are listed on page 22.

DESCRIPTION OF MODELS

The models investigated were designed to study the following end conditions:

Case I – Investigation of a design where all frames were of equal area and bays were of equal length.

Case II – Same as Case I, except that the end bays were shortened by 33 percent in accordance with earlier practice at the Model Basin.

Case III – Same as Case I, except that the end bays were lengthened by 11 percent.

Case IV – The end bays and frames were designed with the maximum principal stress criterion applicable at the bulkheads, but neglecting the beam-column effect resulting from the loads on the ends of the cylinder. End bays were 11 percent longer and end frames were about 20 percent larger than typical ones.

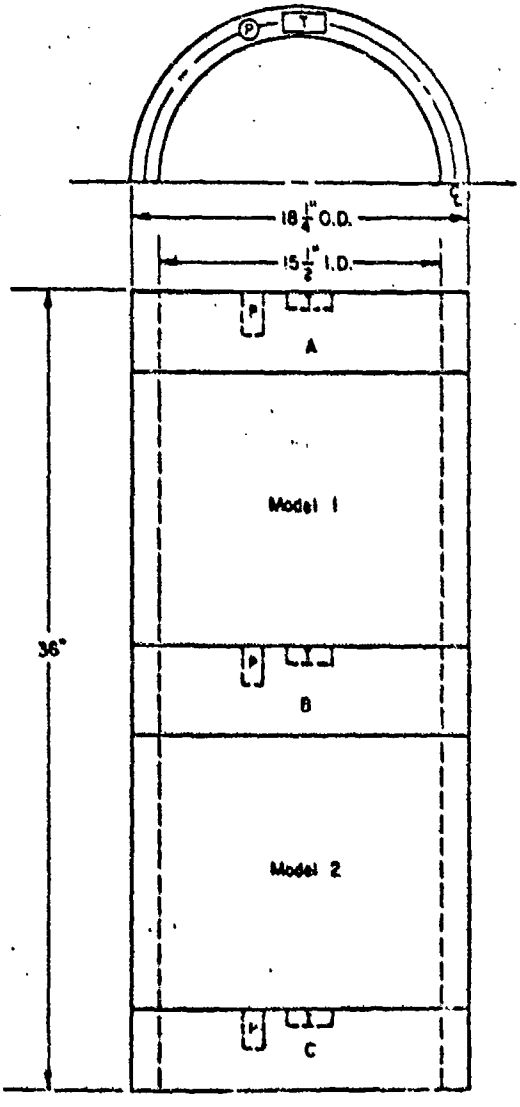

Figure 1 – Diagram of Steel Liner Showing Locations of Identical Models and Yield Specimens

Case V – Investigation of a design in which the beam-column effect was considered. End bays and frames were designed for the same conditions of Case IV. End bays were about 2 percent longer and end frames were 25 percent larger than typical ones.

Case VI – Same as Case V, except that the Hencky-Von Mises yield criterion rather than the maximum principal stress criterion was used as a basis for yielding at the bulkheads.[1] End bays were 8 percent longer and end frames were 23 percent larger than typicals.

To substantiate each collapse pressure, two identical models were machined from a forged steel gun-barrel liner for each of the six different end conditions. The dimensions of a liner and the general location in the liner for identical models are shown in Figure 1. The sections of the liner denoted A, B, and C are regions from which specimens were obtained to determine the yield strength along the length of a liner. The specimens were removed from locations in the liner such that the compressive yield strengths obtained represented the actual yield strengths in the vicinity of the shell of the models. This minimized errors due to variation of yield strength across the thickness of the liner. An average value of yield strength was selected for each model (e.g., for Model EB-1 the average yield strength for the transverse and circumferential directions obtained from Section A and Section B of Figure 1 was adopted as the compressive yield strength).

Model geometries and details of construction are available in Figure 2 and in References 2, 3, and 4; in addition, the yield strengths for the different cases considered are listed in Table 1. However, the following were held constant for all models:

Symbol	Definition	Dimensions
$2R$	Diameter to the median surface of the shell	16.836 in.
h	Shell thickness	0.0858 in.
L_f	Center-to-center distance between adjacent frames, exclusive of the end bays	1.366 in.
d	Overall frame depth	0.5319 in.
A_f	Cross-sectional frame area, exclusive of the end frames	0.0511 in.^{2}

A Young's modulus of 30,000,000 psi and a Poisson's ratio of 0.3 were assumed.

Based on the average compressive yield strength in the twelve models,

$$\text{Average } \lambda \text{ (Thinness factor)} = \sqrt[4]{(L/2R)^2/(h/2R)^3}\ \sqrt{\sigma_y/E} = 0.694$$

where L is the unsupported length of model

E is Young's modulus, and

σ_y is the average compressive yield strength in the shell for the twelve models.

TABLE 1

Yield Strengths of Material

The average yield strength of all models was 66,825 psi.

Case	Model	Yield Strength of Shell Material	
		σ_y psi	Average σ_y for Identical Models psi
I	EB-5	68,830	67,915
	EB-6	67,000	
II	EB-3	65,800	65,900
	EB-4	66,000	
III	EB-7	68,670	68,730
	EB-8	68,790	
IV	EB-1	66,400	66,575
	EB-2	66,750	
V	EB-9	66,750	67,000
	EB-10	67,250	
VI	EB-11	64,830	64,830
	EB-12	64,830	

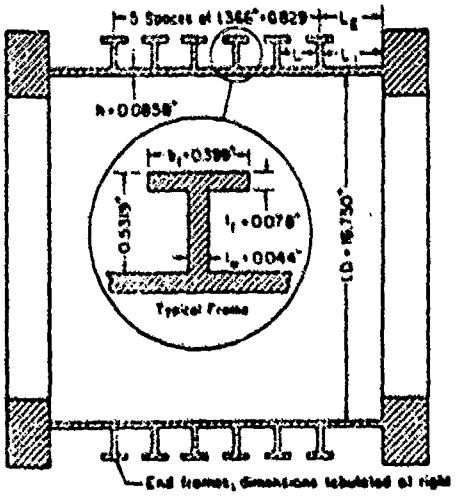

		CASE I	CASE II	CASE III	CASE IV	CASE V	CASE VI
END FRAME	b_f	0.399	0.399	0.399	0.399	0.399	0.399
	t_f	0.078	0.078	0.078	0.095	0.089	0.097
	t_w	0.044	0.044	0.044	0.054	0.057	0.056
L_E		1.344	0.903	1.488	1.493	1.374	1.460
A_1/A^*		1.0	1.0	1.0	1.205	1.250	1.231
L_1/L^{**}		1.0	0.667	1.109	1.109	1.018	1.083

*Ratio of cross-sectional area A_1 of end frame to cross-sectional area A of typical frame.

**Ratio of unsupported length L_1 of end bay to unsupported length L of typical bay.

Figure 2 – Geometric Characteristics of End-Bay Models

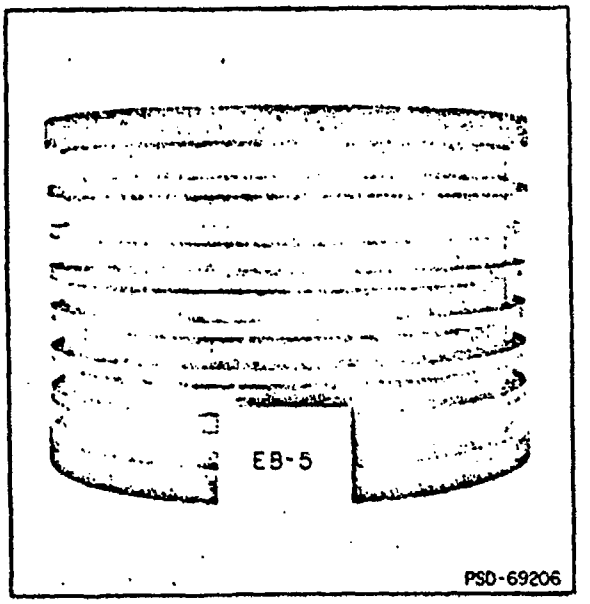

Figure 3 – Typical End-Bay Model

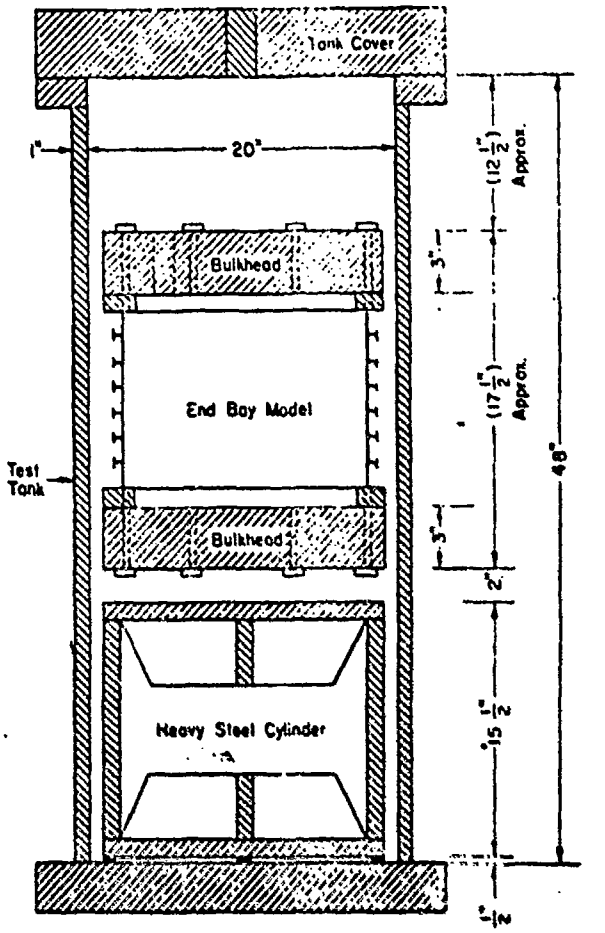

Figure 4 – Schematic Diagram of End-Bay Model Installed in Tank

After each model had been machined, measurements were taken in the laboratory to verify that the model dimensions, i.e., frame dimensions, frame spacing, shell thickness, and inner diameter, conformed with the tolerances specified in References 2 through 4. Afterward, each model together with test specimens obtained from sections adjacent to the model were stress-relieved at 1000° F for one hour and then allowed to air cool. This final step in the fabrication of each model was to obtain stress-free models. On the assumption that machining stresses were the same for model and test specimens, the latter were stress-relieved along with the models to obtain the closest approximation to the compressive yield strength of each model.

The general appearance of a typical end-bay model is shown in Figure 3. Each model had five full-length bays, six T-shaped exterior frames, and two comparatively heavy rectangular end stiffeners; each was machined from a thick tube. The ends of the models were sealed by heavy circular bulkheads shown schematically in Figure 4.

INSTRUMENTATION AND TEST PROCEDURE

Each model was instrumented on the interior and exterior surfaces with SR-4 strain gages to obtain an indication of its behavior under load. In general, Type A-7 gages were used to measure circumferential strains and Type A-8 gages were used to measure longitudinal strains.

Except for Model EB-1 which had gages mounted on four generators of the cylinder, gages were installed along two generators, 180 deg apart. One generator was extensively instrumented adjacent to the heavy end bulkheads and on the centerlines of bays and frames as shown schematically in Table 2. A few selected locations were repeated on the second generator. Variations in the locations of gages from model to model are listed in Table 2. The gage locations were selected to provide the following information:

1. Strain distributions in the end bays to check the strains calculated by the theory described in Reference 1,

2. Strain distributions in the first typical bays for comparison with those for a centrally located typical bay, and

3. Strain distributions in a centrally located bay which is not influenced by the ends of the model.

After each model had been instrumented, all external gages were subjected to a pressure of 1000 psi while the model was free flooded to determine any sensitivity of the gages to pressure. It was assumed that the strain gage was satisfactory when the difference in the strain measurements taken at no load and at 1000 psi was less than 50 μin/in. Those gages measuring strains in excess of 50 μin/in. were replaced.

Each model was tested in the TMB 20-in. diameter, 3000-psi pressure tank. Inasmuch as the volume of the model was small compared with that of the tank, the volume of the tank was reduced to minimize the energy released at failure and, hence, the damage to the models. Volume was reduced by placing a heavy steel cylinder (Figure 4) on the bottom of the tank. Oil was used as the pressure medium.

Two loading runs were conducted for each model in an effort to minimize the nonlinearity of strains and thus ensure a more precise determination of strain-sensitivity factors (the slopes of pressure-strain plots). Pressure increments were measured by means of a 1000-psi Bourdon-tube gage graduated in 5-psi increments. Strains were recorded with Baldwin strain indicators. Loading schedules are given in Table 3.

TEST RESULTS

Experimental collapse pressures are listed in Table 4. Since the yield strengths of the models varied, the collapse pressures of the different models cannot be compared directly with one another until the collapse pressures have been adjusted to a common yield strength. The yield strength selected for this adjustment was the average of all the models. The collapse pressures adjusted to the average yield strength of 66,525 psi are also listed in Table 4.

The mode of failure for each model was identified as axisymmetric yielding evidenced by corrugation of the shell between stiffeners. In each model, deformation occurred very slowly

TABLE 2

Gage Locations for Heavily Instrumented Generator of Models*

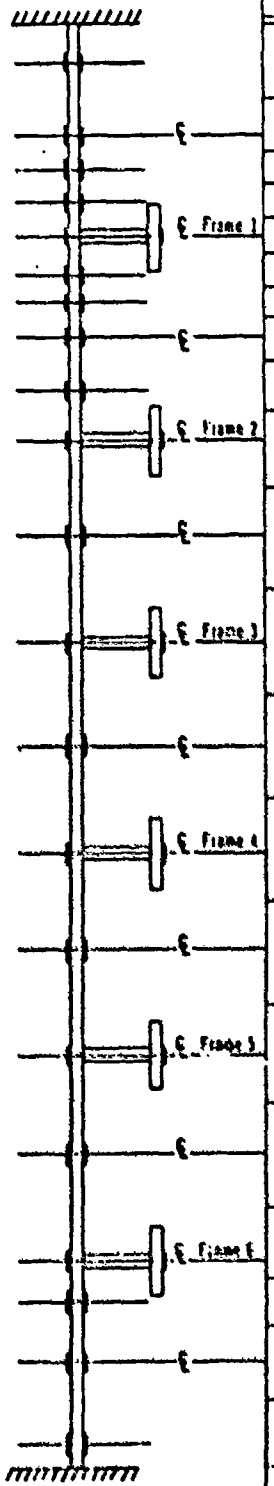

Gage Positions	Ratios of Distances from Nearest Frame or Bulkhead to Frame Spacing											
	EB-1	EB-2	EB-3	EB-4	EB-5	EB-6	EB-7	EB-8	EB-9	EB-10	EB-11	EB-12
1	0.13	0.13	0.21	0.21	0.14	0.14	0.13	0.13	0.14	0.14	0.13	0.13
2	0.50	0.50	0.50		0.50	0.50	0.50	0.50	0.50	0.50	0.50	0.50
3		0.31					0.31		0.31	0.31	0.31	0.31
4	0.13	0.13	0.13		0.13		0.12	0.12	0.13		0.12	0.12
5	0	0	0	0	0	0	0	0	0	0	0	0
6			0.15		0.13		0.13					
7			0.32									
8	0.50	0.50	0.50	0.50	0.50	0.50	0.50	0.50	0.50	0.50	0.50	0.50
9			0.32									
10	0		0		0		0	0	0	0	0	0
11	0.50		0.50		0.50		0.50		0.50	0.50	0.50	0.50
12	0		0		0	0	0	0	0	0	0	0
13	0.50	0.50	0.50	0.50	0.50	0.50	0.50	0.50	0.50	0.50	0.50	0.50
14										0	0	0
15										0.50	0.50	0.50
16										0	0	0
17	0.50		0.50	0.50	0.50	0.50	0.50	0.50	0.50	0.50	0.50	0.50
18	0		0	0	0	0	0	0	0	0	0	0
19								0.12				
20					0.50		0.50	0.50		0.50	0.50	0.50
21	0.13		0.21	0.21	0.14		0.13		0.14			

*A few gages were located at various points on other generators for check purposes.

TABLE 3 – Loading Schedules

Pressures at Which Strains Were Measured, psi			
Models EB-1 through EB-10		Model EB-11 and 12	
Run 1	Run 2	Run 1	Run 2
0	0	0	0
100	300	200	300
200	600	400	600
300	700	500	700
400	800	600	800
500	825*	0	850
600	850		900
0	875**		920
	925 †		940
	950 ††		

*Applicable only for Model EB-6.

**Applicable only for Models EB-4 and EB-10.

†Not applicable for Models EB-3 and EB-9.

††Not applicable for Models EB-3, 4, 6, 7, and 9.

TABLE 4 – Summary of Experimental and Theoretical Collapse Pressures

Model	Experimental Collapse Pressure, psi		Case	Failure Areas	Averaged Experimental Collapse Pressure psi	Experimental Collapse Pressure / Theoretical Collapse Pressure	
	Actual	Corrected to σ_y = 66,825 psi				HVM Criterion Midbay Midplane	Plastic Hinge Theory
EB-5	960	932	I	First Typical Bay	940	0.934	0.967
EB-6	950	948					
EB-3	921	935	II	First Typical Bay	936	0.931	0.963
EB-4	925	937					
EB-7	955	929	III	End Bay	933	0.928	0.960
EB-8	965	937					
EB-1	975	982	IV	End Bay	979	0.973	1.008
EB-2	975	976					
EB-9	950	951	V	Second Typical Bay	948.5	0.943	0.976
EB-10	952	946					
EB-11	950	979	VI	Second Typical Bay	964	0.978	1.013
EB-12	960	989					

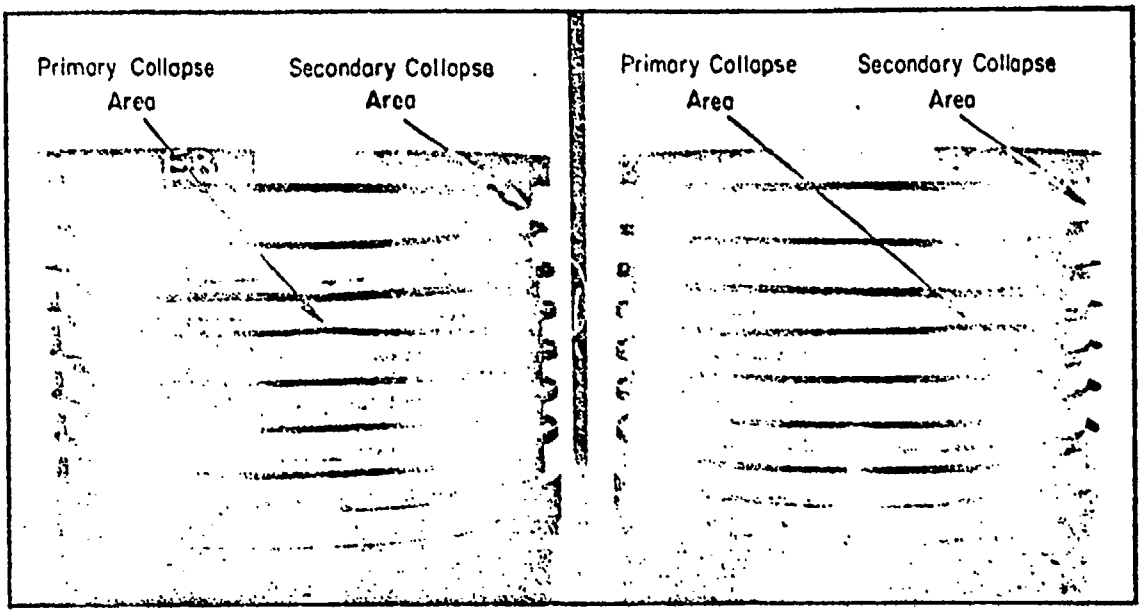

Figure 5 – Identical Models EB-11 and EB-12 (Case VI) After Collapse

with practically no noise and extended about 90 deg around the model. Failure modes were identical in form and in general location for identical models as shown, for example, in Figure 5. Failures located in an end bay (Case IV), in a first typical bay (Case I), and in a second typical bay (Case V) are shown in Figure 6. Case V models had visible damage in the first typical bays, but, like Case VI models, they failed initially in the second typical bay.

Strain-sensitivity factors in microinches per inch per psi of pressure are given in Tables 5 through 7. The circumferential strain-sensitivity factors in Table 5 are averaged values for the interior and exterior surfaces, and, in general, the factors have been averaged for duplicate longitudinal locations (where strains were measured on two generators). Typical pressure-strain curves from which these sensitivity factors were obtained are shown in the Appendix.

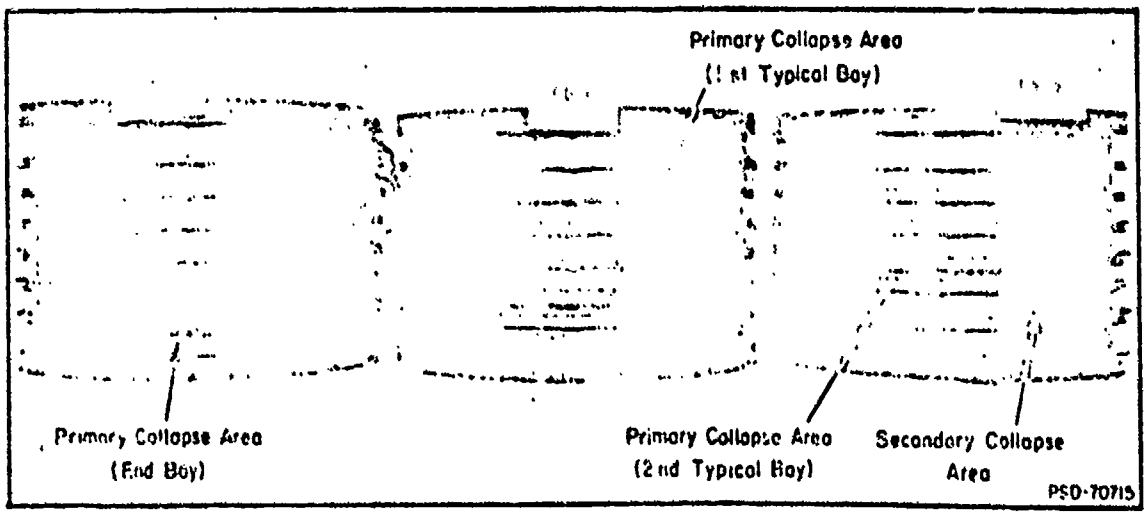

Figure 6 – Models EB-2, EB-6, EB-9 After Collapse

TABLE 5

Experimental Circumferential Strain-Sensitivity Factors

General Location	Distance (x/L) in Terms of Bay Length	Strain-Sensitivity Factors, μ in/psi											
		Case IV		Case II		Case I		Case III		Case V		Case VI	
		EB-1	EB-2	EB-3	EB-4	EB-5	EB-6	EB-7	EB-8	EB-9	EB-10	EB-11	EB-12
Upper End Bay	0.13	−0.30	+0.01	−0.05	−0.09	−0.14	−0.07	−0.12	−0.33	−0.30	−0.44	−0.30	−0.47
	0.21												
	0.50	−1.25		−0.53		−1.09	−0.96	−1.20	−1.32	−1.13	−1.21	−1.26	−1.39
	0.69	−1.80	−1.31					−1.53		−1.39	−1.45	−1.52	−1.63
	0.78	−1.90		−0.91									
	0.87		−1.42			−1.64		−1.78	−1.84	−1.30		−1.63	−1.74
First Frame	1.00	−1.75	−1.63	−1.24	−1.44	−1.75	−1.69	−1.80	−1.83	−1.59	−1.62	−1.63	−1.64
First Typical Bay	0.13												
	0.15					−2.03							
	0.32			−1.79									
	0.50	−2.14	−1.83	−2.02	−2.01	−2.11	−1.99	−2.00	−2.08	−1.95	−1.97	−1.99	−1.97
	0.68			−2.00									
Second Frame	1.00	−1.85		−1.71		−1.76		−1.75	−1.76	−1.68	−1.81	−1.72	−1.73
Bay	0.50	−2.11		−1.82		−1.99		−1.94		−1.92	−1.99	−1.98	−1.94
Third Frame	1.00	−1.77		−1.84		−1.73	−1.60	−1.78	−1.76	−1.59	−1.76	−1.72	−1.72
Bay	0.50	−2.08	−1.90	−1.88	−1.98		−1.90	−1.98	−2.06	−1.93	−2.00	−2.00	−1.99
Fourth Frame	1.00										−1.78	−1.68	−1.73
Bay	0.50										−1.98	−1.98	−1.90
Fifth Frame	1.00										−1.78	−1.72	−1.66
Bay	0.50	−2.09		−2.07	−2.02	−2.05	−2.06	−2.16	−2.07	−1.95	−2.06	−1.80	−1.98
Sixth Frame	1.00	−1.80		−1.34	−1.30	−1.72	−1.71	−1.84	−1.81	−1.59	−1.63	−1.69	−1.67
Lower End Bay	0.12												
	0.50					−1.25		−1.50	−1.75		−1.12	−1.20	−1.38
	0.79			−0.63									
	0.86	−0.31		0	−0.40	−0.53		−0.45		−0.14			

TABLE 6

Experimental Longitudinal Strain-Sensitivity Factors (Exterior Surface)

General Location	Distance (x/L) in Terms of Bay Length	Strain-Sensitivity Factors, μ in/psi											
		Case IV		Case II		Case I		Case III		Case V		Case VI	
		EB-1	EB-2	EB-3	EB-4	EB-5	EB-6	EB-7	EB-8	EB-9	EB-10	EB-11	EB-12
Upper End Bay	0.13	+1.64	+1.21	N.G.	+0.39	–	+0.50	+0.47	+0.61	+0.50	+0.52	+0.45	+0.54
	0.21												
	0.50	-1.79	-2.33	-1.32		-1.73	-2.04	-2.63	-1.87	-1.68	-1.62	-2.04	-1.93
	0.69	-0.99	-2.11					-2.49		-1.79	-1.94	-1.73	-1.84
	0.78			-1.25									
	0.87		-1.83			-1.30		-1.51	-1.23	-1.34		-0.98	-0.71
First Frame	1.00												
First Typical Bay	0.13												
	0.15												
	0.32												
	0.50	-1.35	-1.59	-1.99	-1.37	-1.37		-1.65	-1.13	-1.26	-1.33	-1.37	-1.04
	0.68												
Second Frame	1.00												
Bay	0.50	-1.24		-1.63		-1.09		-1.40		-1.06	-1.18	-1.34	-1.20
Third Frame	1.00												
Bay	0.50	-1.08	-1.37	-1.52	-1.26	-1.23	-1.40	-1.35	-1.06	-1.25	-1.15	-1.29	-1.28
Fourth Frame	1.00												
Bay	0.50										-1.22	-1.30	-1.16
Fifth Frame	1.00												
Bay	0.50	-1.26		-1.80	-2.05	-1.23	-1.37	-1.11	-1.04	-1.31	-1.48	-1.44	-1.19
Sixth Frame	1.00												
Lower End Bay	0.12								-0.81				
	0.50					-1.07		-1.68	-1.46		-1.51	-2.15	-2.04
	0.79												
	0.86	+0.37		+0.55	+0.40			+0.71		+0.61			

TABLE 7

Exporimental Longitudinal Strain-Sensitivity Factors (Interior Surface)

General Location	Distance (x/L) in Terms of Bay Length	Strain-Sensitivity Factors, μin/psi											
		Case IV		Case II		Case I		Case III		Case V		Case VI	
		EB-1	EB-2	EB-3	EB-4	EB-5	EB-6	EB-7	EB-8	EB-9	EB-10	EB-11	EB-12
Upper End Bay	0.13	-2.55	-3.97	-3.54	-2.23	-2.80	-4.57	-4.10	-2.26	-1.70	-1.56	-2.60	-2.45
	0.21												
	0.50	+0.16	-0.25	-1.60		-0.15	-0.66	-0.42	-0.03	-0.08	-0.08	+0.08	-0.19
	0.69	+0.25	-0.15							-0.08	-0.08		+0.17
	0.78			-1.11									
	0.87	+0.24	-0.85			-0.31		-0.63	-0.57	-0.79		-0.46	-0.60
First Frame	1.00	-1.30	-1.21	-1.15	-0.71	-1.25	-1.33	-1.53	-1.16	-1.37	-1.28	-1.58	
First Typical Bay	0.13					-0.28		-1.22					
	0.15			-0.57									
	0.32			-0.23									
	0.50	-0.20	-0.37	-0.16	+0.33	-0.23	-0.26	-0.41	-0.21	-0.10	-0.15	-0.21	-0.20
	0.68			-0.46									
Second Frame	1.00	-1.56		-2.13		-1.25		-1.94	-1.67	-1.13	-1.72	-1.71	
Bay	0.50	-0.35		-0.60		-0.31		-0.47		-0.25	-0.35	-0.38	-0.36
Third Frame	1.00	-1.45		-2.05		-1.30	-1.83		-1.61	-1.03	-1.75	-1.76	-1.77
Bay	0.50	-0.30	-0.37	-0.47	-0.32	-0.28	-0.36	-0.35	-0.24	-0.31	-0.36	-0.34	-0.32
Fourth Frame	1.00										-1.80	-1.78	-1.74
Bay	0.50										-0.33	-0.35	-0.37
Fifth Frame	1.00										-1.70	-1.83	-1.71
Bay	0.50	-0.05		+0.16	+0.30	+0.10	-0.02	-0.06	-0.05	-0.10	-0.13	-0.23	-0.24
Sixth Frame	1.00	-1.00		-1.05	-1.25	-1.36	-1.02	-1.05	-0.88	-1.34	-1.46	-1.60	-1.58
Lower End Bay	0.12					-0.11		+0.45	+0.13		-0.23	+0.13	+0.11
	0.50								+0.19				
	0.79									-3.50			
	0.86	-2.43			-3.62	-2.50		-2.87					

COMPARISON OF EXPERIMENT WITH THEORY

Experimental collapse pressures are compared with theoretical pressures in Table 4. Criteria for shell yield considered most applicable for this failure mode are the Hencky-Von Mises criterion[5] for a midplane point at midbay and the plastic-hinge theory.[6] For the geometry investigated, the first theory gave a pressure of 1006 psi and the plastic-hinge theory gave a value of 972 psi. Ratios of experimental pressures corrected for the average yield strength (66,825 psi) to these theoretical pressures are given in Table 4.

Of all the models tested, those of Case VI collapsed at pressures agreeing best with pressure computed by the Hencky-Von Mises membrane-stress method (within 2½ percent). The experimental pressures for Case VI models were also in close agreement with the pressures computed by the plastic hinge theory (within 1½ percent). Although the experimental collapse pressures of Case IV agreed well with pressures computed by the plastic hinge methods, the design procedure for this case is less rigorous than that for the Case VI models. Therefore, the Case VI procedure is recommended.

Strains measured for Case VI models are compared in Figure 7 with strains determined by the theory of Reference 1. Two theoretical curves are shown: one for the elastic strain sensitivities before yielding occurs at the bulkheads (obtained for a pressure equal to 200 psi), and the other for strain sensitivities after yielding at the bulkheads and near collapse pressure (obtained for a pressure equal to 920 psi). The experimental strains shown are averaged values for Models EB-11 and EB-12.

Experimental circumferential strains in the end bays are higher than theoretical strains in the elastic range and lower in the yield range as shown in Figures 7a and 7b. Nevertheless, agreement between theory and experiment is good. Comparison of longitudinal strains on the exterior surface (Figure 7c) indicates that experimental strains in the end bays are slightly less than the theoretical strains in the elastic range, but they are larger than calculated strains in the yield range. In Figure 7d, the experimental longitudinal strains on the interior shell surface appear to be generally lower than calculated strains. However, in general for Figures 7a through 7d the plotted experimental points agree well with the curve of theoretical strain along the length of the models.

DISCUSSION OF RESULTS

Test results obtained from this series of models were consistent. The maximum difference between collapse pressures for identical pairs of models was 1 percent; the overall change in model strength imposed by the varying end conditions was on the order of 5 percent. Also, for all models, the mode of failure was identical as was the bay of failure for identical models; hence, the mode of failure was clearly established for each case. Models tested for the first three cases, where all frames were of equal area and the end-bay lengths varied, were about 5 percent weaker than Case VI models. Increasing the size of the end frames together

Figure 7 – Comparison of Theoretical Strain Distribution with Experimental Strain Distribution for Models in Case VI

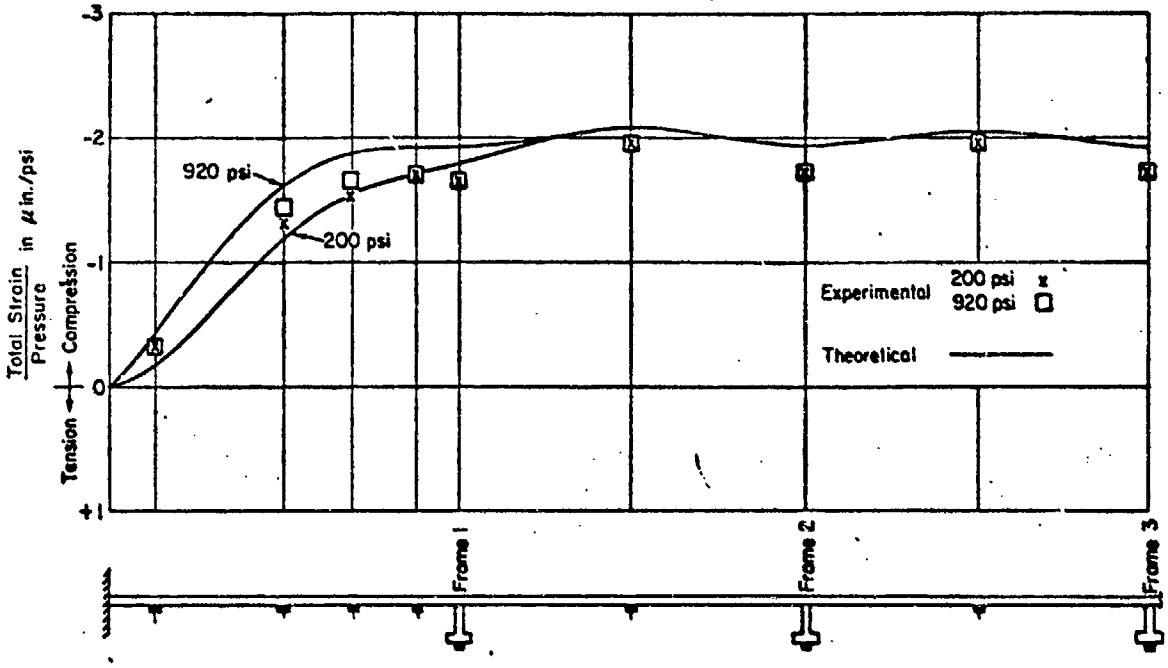

Figure 7a – Circumferential Strains, Exterior Surface

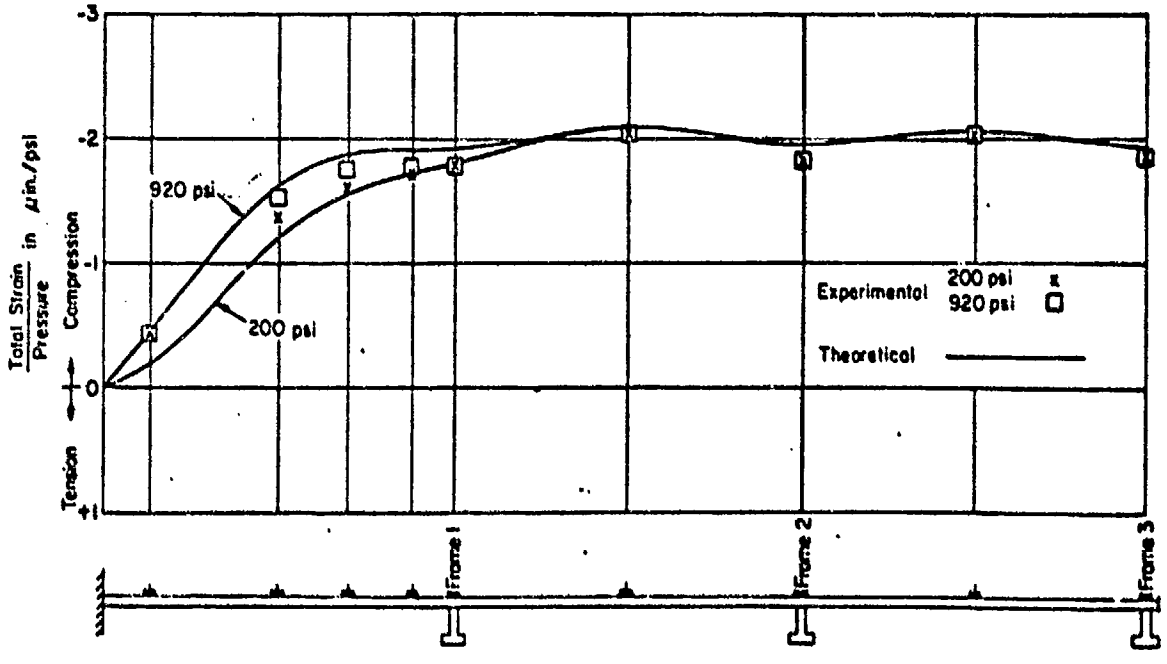

Figure 7b – Circumferential Strains, Interior Surface

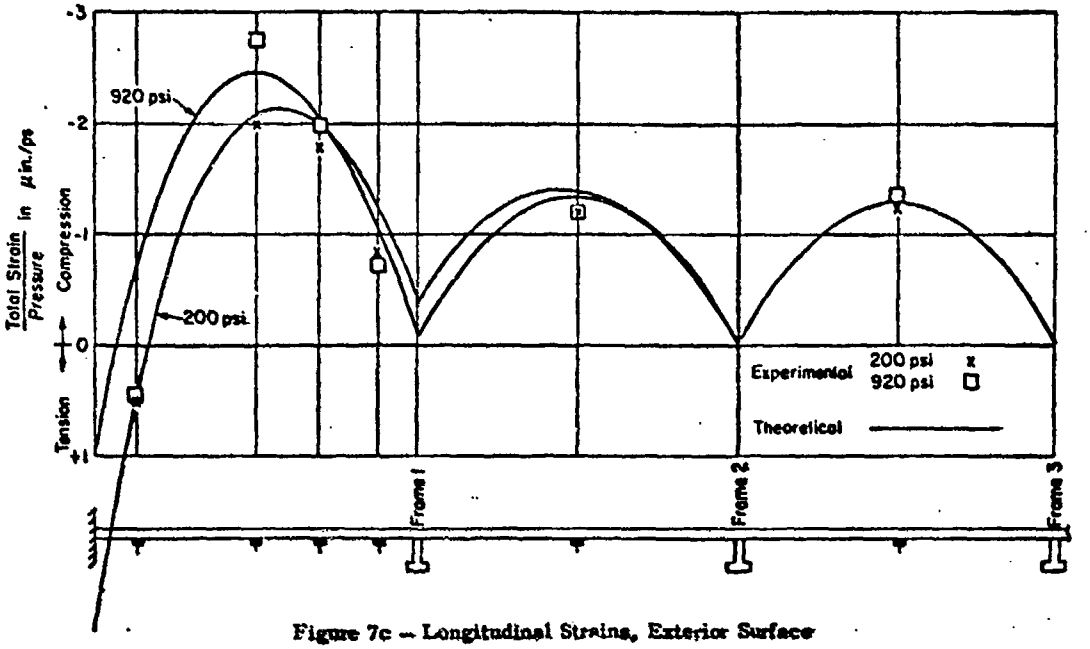

Figure 7c – Longitudinal Strains, Exterior Surface

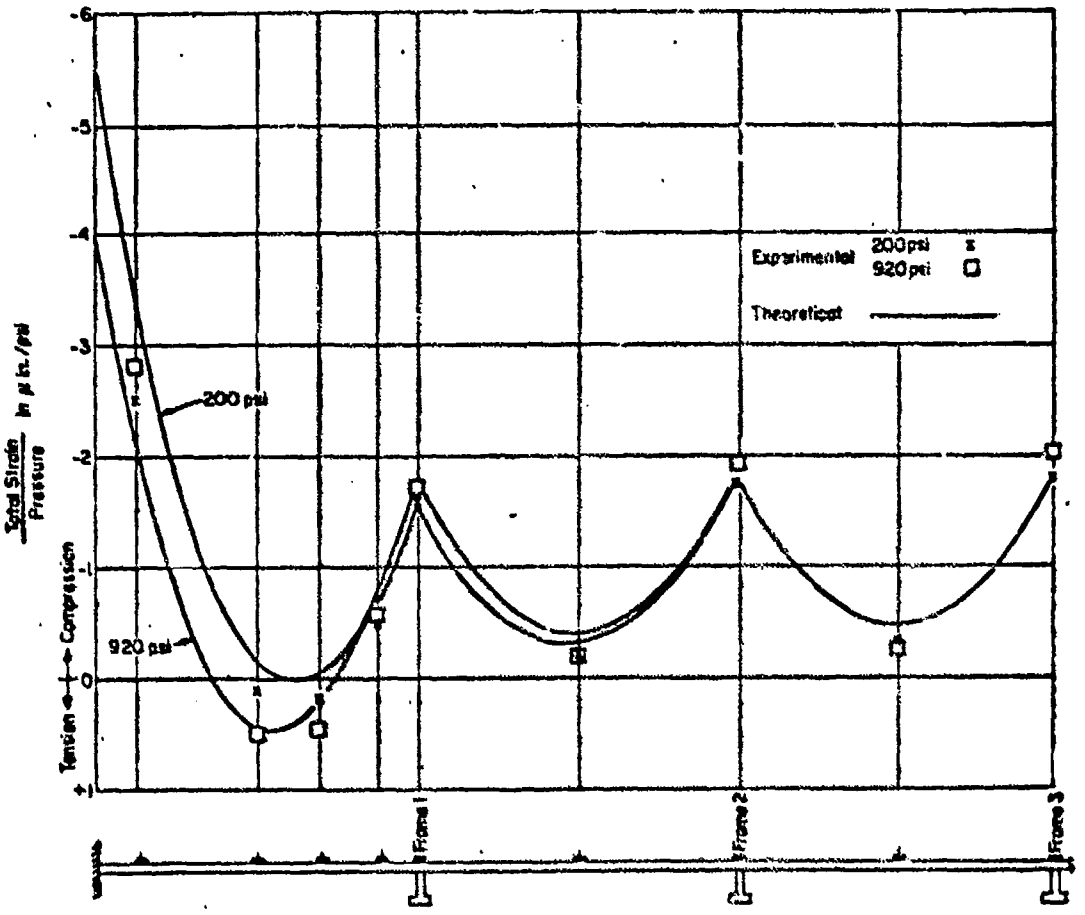

Figure 7d – Longitudinal Strains, Interior Surface

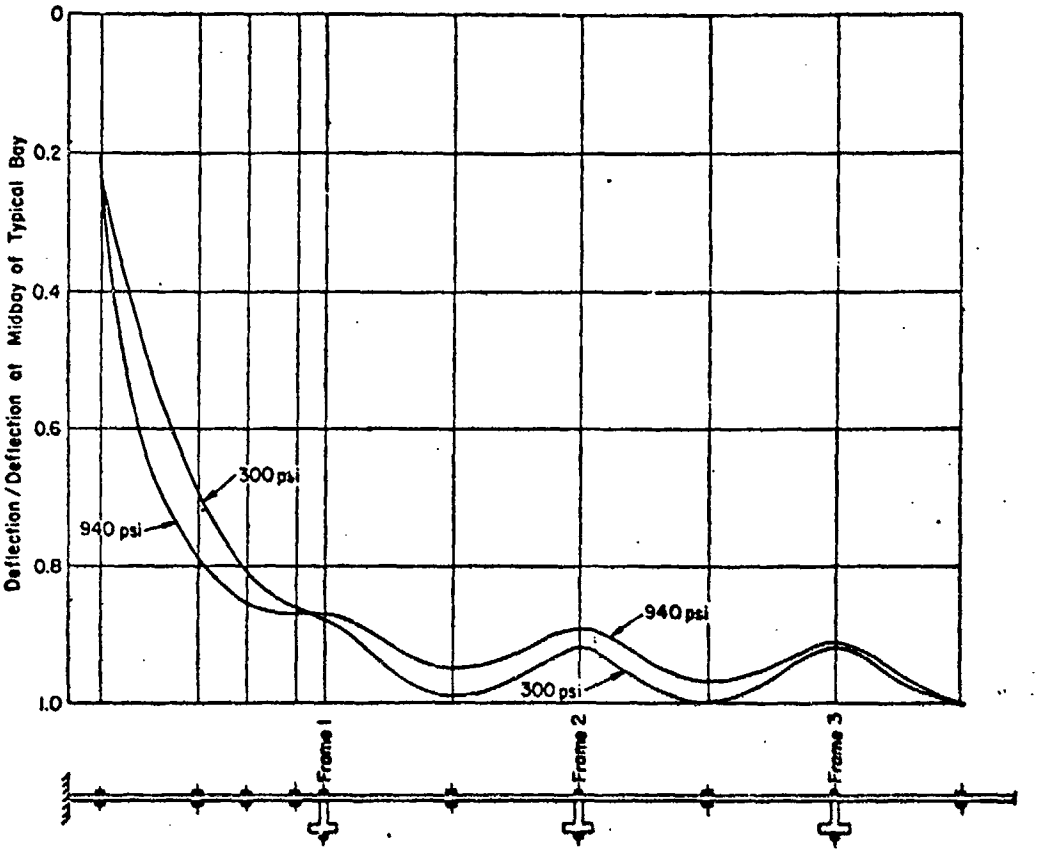

Figure 8 – Deflection Pattern for Case VI (Models EB-11 and 12)

with selecting endbay spacing based on theoretical considerations for the remaining Cases (IV, V, VI) resulted in increased collapse pressures.

The good agreement between the collapse pressures for the models of Case VI and the theoretical pressures can be attributed to having designed the models to conform with the assumptions of the optimum design procedures of Reference 1. (For Case VI, the beam-column effect is taken into account and the Hencky-Von Mises criterion of yielding is assumed at the bulkheads.) Case VI models and Case IV models were stronger (by 3.7 and 3.2 percent, respectively), than Case V models. (For Case V, the beam-column effect is also considered, but the maximum stress criterion is assumed at the bulkheads. For Case IV the beam-column effect is neglected and only the maximum stress criterion is considered.)

Experimental strain sensitivities for Models EB-11 and EB-12 for both the elastic range and just prior to collapse are shown in Figure 7. They agree favorably with the theoretical curves computed using the end-bay theory.[1] Discrepancies between the assumed properties (Poisson's ratio and modulus of elasticity) and those actually existing in the material of the models are probably partly responsible for the difference between theory and experiment in the typical bays.

Figure 8 indicates for the optimum end-bay design (Case VI) how the deflections at the ends of the model compare with those at the middle of the centrally located bay which is least

disturbed by the ends of the model. It should be noted that prior to yielding at the bulkhead at 300 psi Frames 2 and 3 deflected about the same whereas after yielding at the bulkhead at 940 psi Frame 3 has deflected more than Frame 2. Also, it should be noted that at the pressure (940 psi) approaching the collapse pressure, Frames 2 and 3 deflected less than at 300 psi as did the shell between Frames 1 and 2 and Frames 2 and 3. At the higher pressure the deflections in none of the bays exceeded that of the central bay. It will also be noticed that deflections of Frames 1 and 2 which are quite different in the elastic range tend to equalize at the higher pressure where plastic action occurs at the bulkhead as assumed in the theory.

CONCLUSIONS

Test results lead to the following conclusions:

1. The theory for optimum end-bay design is confirmed experimentally in Case VI. For the geometries tested, the end bay determined by the optimum design procedure is 5 percent stronger than an end bay arbitrarily selected as two-thirds of a typical bay.

2. The strains at the ends of a cylinder can be determined accurately by the end-bay theory. The tests of the optimum design confirm the theoretical results which indicate that the deflections of the first and second frames are different in the elastic range but tend to become equal after yielding occurs at the bulkheads.

3. Where the end-bay design is optimum, failure can occur in bays other than the end bay or first typical bay.

4. The collapse pressure for models with ends of optimum design is closely predicted with the plastic hinge theory.

RECOMMENDATIONS

It is recommended that theoretical work be continued to develop an end-bay design procedure in which the length of the end bay is varied with the shell thickness of this bay rather than with the size of the first frame.

ACKNOWLEDGMENTS

The authors wish to express their thanks to LT William E. Trueblood, USN, and James A. Nott for testing some of the earlier models in this series. They are also indebted to Robert D. Short for his advice and assistance during the course of the tests. The authors wish also to express their appreciation to Dr. M.E. Lunchick for his guidance during the original planning and his assistance in preparing this report.

APPENDIX

PRESSURE-STRAIN PLOTS

Accumulated strain was plotted at each pressure increment with pressure as the ordinate and strain as the abscissa. Sample plots are presented in Figures 9 and 10. Since the permanent set was practically zero for the first run, only one curve is shown for both the first and second runs. The number in parentheses on each pressure-strain curve is the strain-sensitivity factor.

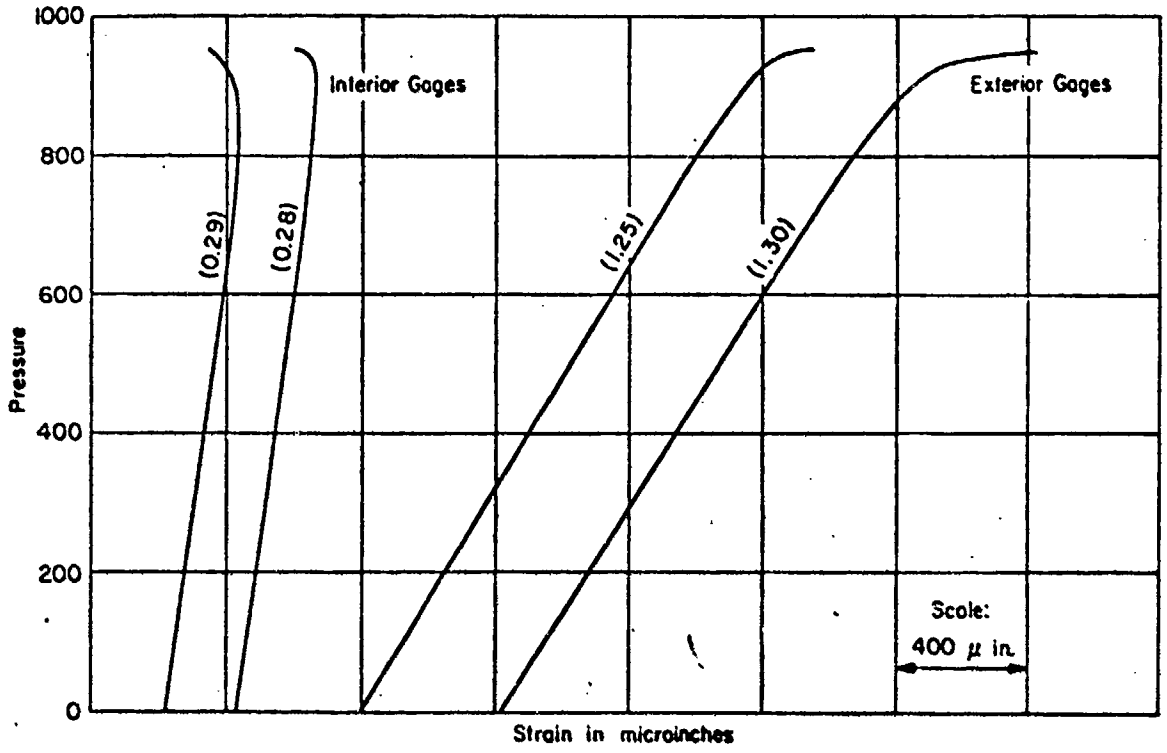

Figure 9a – Longitudinal Gages

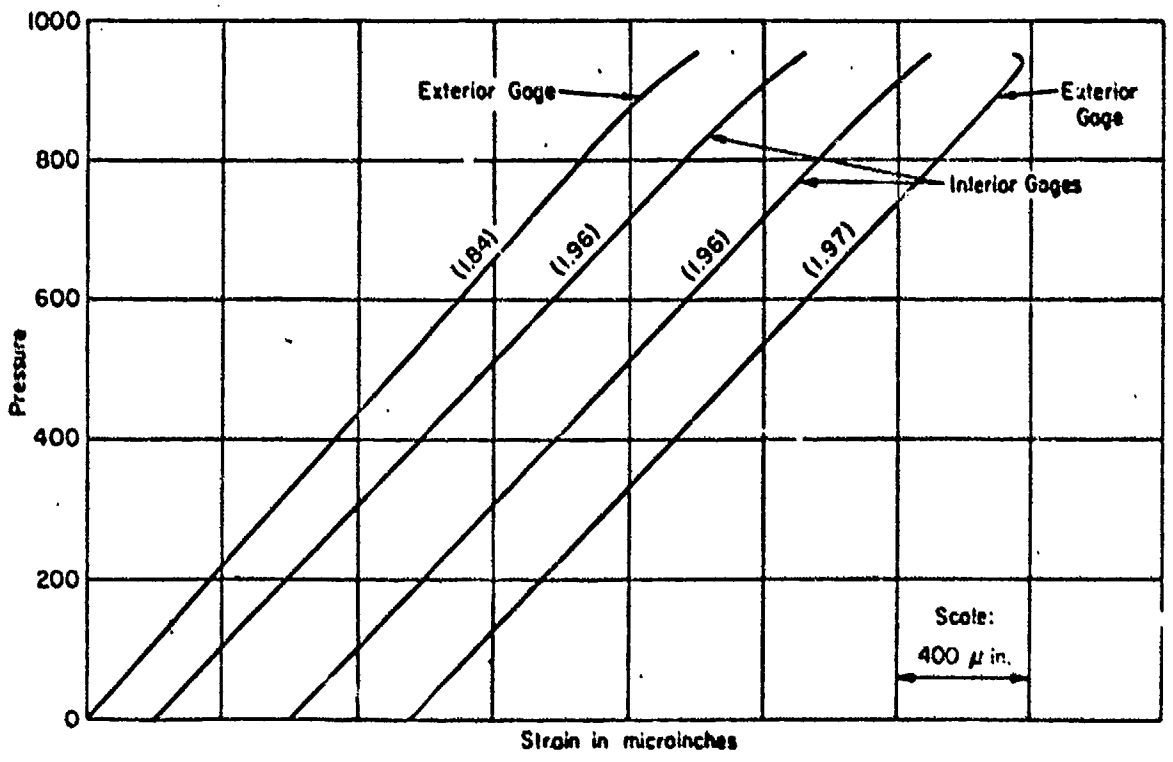

Figure 9b – Circumferential Gages

Figure 9 – Pressure-Strain Plots for Gages Mounted Midbay in Center Bay of Model EB-12

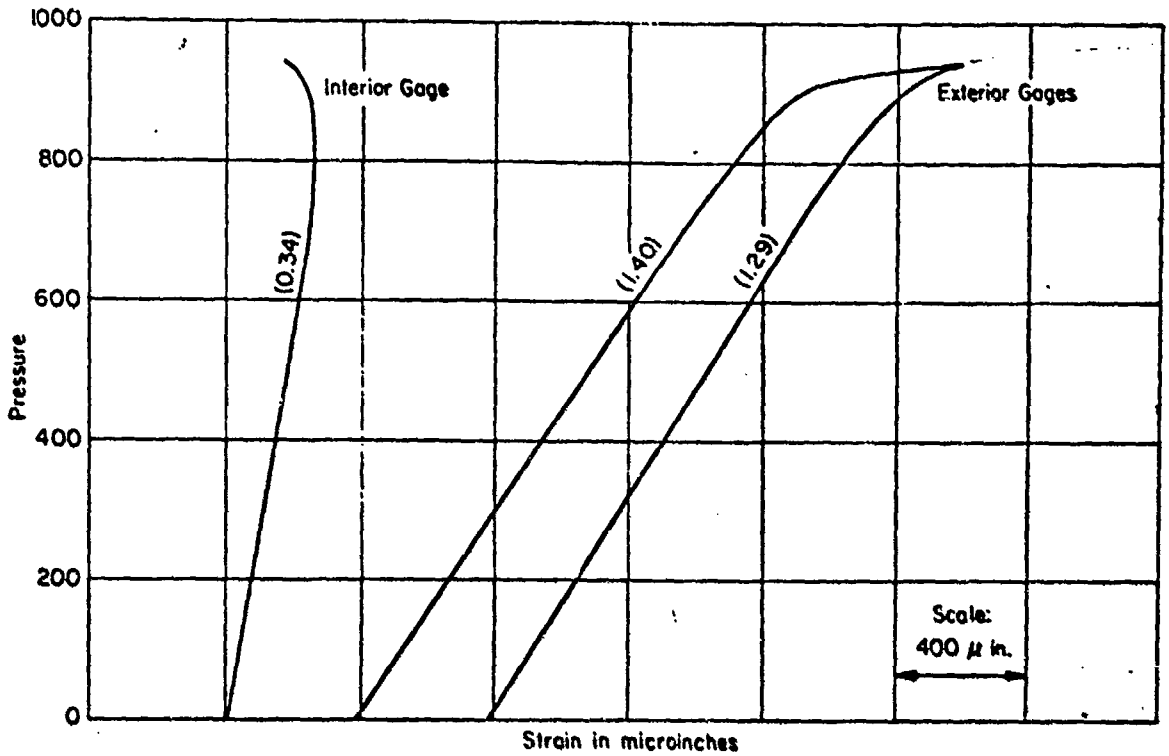

Figure 10a – Longitudinal Gages

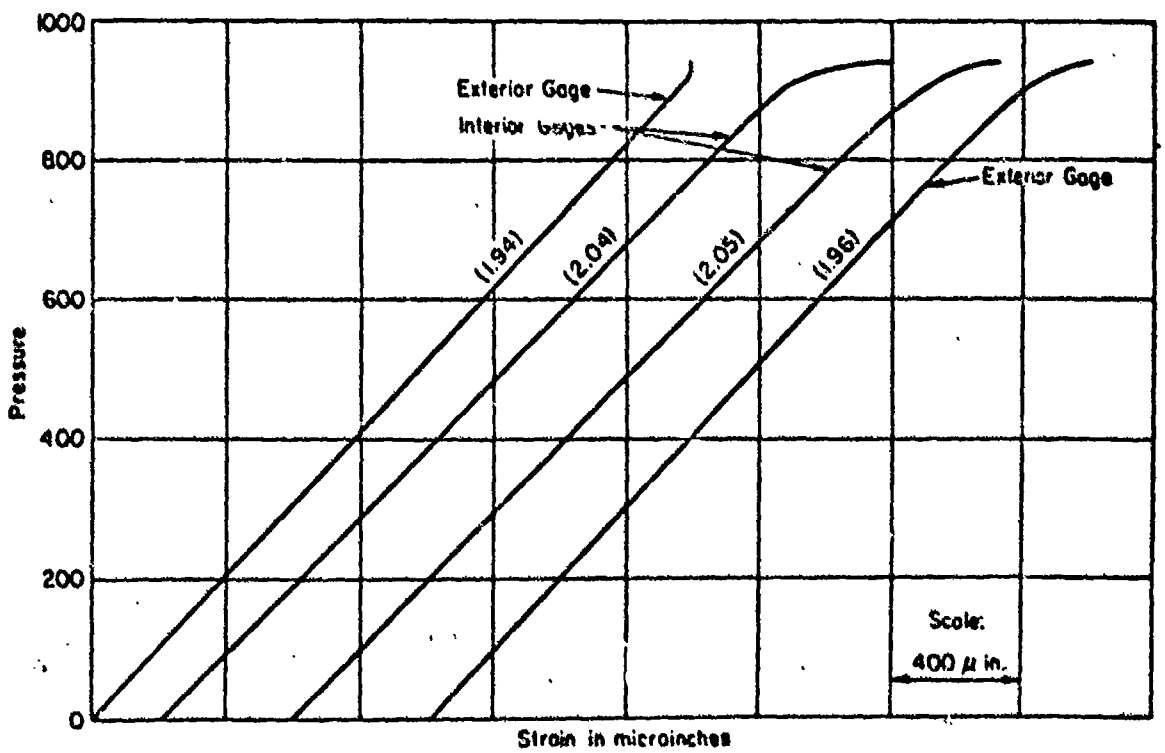

Figure 10b – Circumferential Gages

Figure 10 – Pressure-Strain Plots for Gages Mounted Midbay in Center Bay of Model EB-11

REFERENCES

1. Short, R.D. and Bart, R., "The Effects of End Conditions on the Stresses in Stiffened Cylindrical Shells," David Taylor Model Basin Report 1065 (Jun 1959).

2. David Taylor Model Basin Drawing C-114-1 "E.B. Machined Models," (Mar 1957).

3. David Taylor Model Basin Drawing C-114-2 "E.B. Machined Models 9 and 10," (Aug 1957).

4. David Taylor Model Basin Drawing C-114-3 "E.B. Machined Models 11 and 12," (May 1958).

5. Timoshenko, S. and MacCullough, G.H., "Elements of Strength of Materials," D. Van Nostrand Company, Inc., New York, Second Edition, p. 325 (1946).

6. Lunchick, M.E., "Yield Failure of Stiffened Cylinders under Hydrostatic Pressure," Proceedings of Third U.S. National Congress of Applied Mechanics, pp. 589-594 (1958).

INITIAL DISTRIBUTION

Copies	
13	CHBUSHIPS 3 Tech Info Sec (Code 335) 1 Tech Asst (Code 106) 1 Prelim Design Br (Code 420) 1 Prelim Design Sec (Code 421) 1 Ship Pro Sec (Code 423) 1 Hull Design Br (Code 440) 2 Sci & Res Sec (Code 442) 1 Structure (Code 443) 1 Submarines (Code 525) 1 Hull Arr, Struc, & Preserv Br (Code 633)
3	CHONR 1 Fluid Dyn Br (Code 438) 1 Struc Mech Br (Code 439) 1 Undersea Warfare Br (Code 466)
1	CNO (Op 311)
1	CDR, USNOL
1	DIR, USNRL, Attn: TID
2	NAVSHIPYD PTSMH
2	NAVSHIPYD MARE
1	NAVSHIPYD NORVA, UERD (Code 280)
1	SUPSHIPINSORD, Groton
1	Electric Boat Div, Gen Dynamics Corp.
1	SUPSHIPINSORD, Newport News
1	Newport News Shipbuilding & Dry Dock Co.
1	SUPSHIPINSORD, Pascagoula
1	Ingalls Shipbuilding Corp.
1	SUPSHIPINSORD, Camden
1	New York Shipbuilding Corp.
1	Dir of Defense, R & E, Attn: Tech Library
1	CO, USNROTC & NAVADMINU MIT
1	O in C, PGSCOL, Webb

David Taylor Model Basin. Report 1326.
AN EXPERIMENTAL INVESTIGATION OF EFFECT OF END CONDITIONS ON STRENGTH OF STIFFENED CYLINDRICAL SHELLS, by R.F. Keefe and J.A. Overby. December 1959. iii, 23p. illus., photos., graphs, tables, refs. UNCLASSIFIED

Six pairs of stiffened cylinders, machined from thick tubes and identical except for the size and spacing of the frames at the ends, were subjected to external hydrostatic pressure to establish the adequacy of a design procedure for the end bays. All the cylinders failed by axisymmetric shell yielding, four in the end bay, four in the first full-length bay, and four in the second full-length bay. For each pair of identical cylinders, the locations of damage at failure were identical and the collapse pressures differed by less than 1 percent when adjusted to a common yield

1. Cylindrical shells (Stiffened) – Failure
2. Cylindrical shells (Stiffened) – Stresses
I. Keefe, Robert F.
II. Overby, James A.
III. NS731-038

David Taylor Model Basin. Report 1326.
AN EXPERIMENTAL INVESTIGATION OF EFFECT OF END CONDITIONS ON STRENGTH OF STIFFENED CYLINDRICAL SHELLS, by R.F. Keefe and J.A. Overby. December 1959. iii, 23p. illus., photos., graphs, tables, refs. UNCLASSIFIED

Six pairs of stiffened cylinders, machined from thick tubes and identical except for the size and spacing of the frames at the ends, were subjected to external hydrostatic pressure to establish the adequacy of a design procedure for the end bays. All the cylinders failed by axisymmetric shell yielding, four in the end bay, four in the first full-length bay, and four in the second full-length bay. For each pair of identical cylinders, the locations of damage at failure were identical and the collapse pressures differed by less than 1 percent when adjusted to a common yield

1. Cylindrical shells (Stiffened) – Failure
2. Cylindrical shells (Stiffened) – Stresses
I. Keefe, Robert F.
II. Overby, James A.
III. NS731-038

David Taylor Model Basin. Report 1326.
AN EXPERIMENTAL INVESTIGATION OF EFFECT OF END CONDITIONS ON STRENGTH OF STIFFENED CYLINDRICAL SHELLS, by R.F. Keefe and J.A. Overby. December 1959. iii, 23p. illus., photos., graphs, tables, refs. UNCLASSIFIED

Six pairs of stiffened cylinders, machined from thick tubes and identical except for the size and spacing of the frames at the ends, were subjected to external hydrostatic pressure to establish the adequacy of a design procedure for the end bays. All the cylinders failed by axisymmetric shell yielding, four in the end bay, four in the first full-length bay, and four in the second full-length bay. For each pair of identical cylinders, the locations of damage at failure were identical and the collapse pressures differed by less than 1 percent when adjusted to a common yield

1. Cylindrical shells (Stiffened) – Failure
2. Cylindrical shells (Stiffened) – Stresses
I. Keefe, Robert F.
II. Overby, James A.
III. NS731-038

David Taylor Model Basin. Report 1326.
AN EXPERIMENTAL INVESTIGATION OF EFFECT OF END CONDITIONS ON STRENGTH OF STIFFENED CYLINDRICAL SHELLS, by R.F. Keefe and J.A. Overby. December 1959. iii, 23p. illus., photos., graphs, tables, refs. UNCLASSIFIED

Six pairs of stiffened cylinders, machined from thick tubes and identical except for the size and spacing of the frames at the ends, were subjected to external hydrostatic pressure to establish the adequacy of a design procedure for the end bays. All the cylinders failed by axisymmetric shell yielding, four in the end bay, four in the first full-length bay, and four in the second full-length bay. For each pair of identical cylinders, the locations of damage at failure were identical and the collapse pressures differed by less than 1 percent when adjusted to a common yield

1. Cylindrical shells (Stiffened) – Failure
2. Cylindrical shells (Stiffened) – Stresses
I. Keefe, Robert F.
II. Overby, James A.
III. NS731-038